

doi: 10.12029/gc20160505

冯光英, 杨经绥, 刘飞, 等. 新疆中天山干沟一带晚石炭世花岗岩的岩石成因及其地质意义[J]. 中国地质, 2016, 43(5): 1545–1557.

Feng Guangying, Yang Jingsui, Liu Fei, et al. Petrogenesis and geological significance of the Late Carboniferous granites from Gangou, Central Tianshan Mountains, Xinjiang[J]. *Geology in China*, 2016, 43(5): 1545–1557(in Chinese with English abstract).

## 新疆中天山干沟一带晚石炭世花岗岩的岩石成因 及其地质意义

冯光英<sup>1</sup> 杨经绥<sup>1</sup> 刘飞<sup>1</sup> 牛晓露<sup>1</sup> 高健<sup>2</sup>

(1. 中国地质科学院地质研究所, 地幔研究中心, 北京 100037; 2. 昆明理工大学, 云南 昆明 650504)

**摘要:** 中天山干沟一带花岗岩广泛分布, 前人对北部的眼球状花岗岩和细粒花岗岩进行了精确的 SHRIMP 定年研究, 其侵位年龄分别为 428 Ma 和 361~368 Ma, 笔者对干沟南部的晚石炭世花岗岩进行了锆石 LA-ICP-MS U-Pb 定年研究, 其侵位年龄为(301.2±1.0) Ma。干沟晚石炭世花岗岩属于高钾钙碱性系列, 其 $\sigma$ 值为 2.6~3.22, 显示钙碱性与碱性过渡的特点, 富集轻稀土元素及 Rb、K、Th、La 及高场强元素 Zr 和 Hf, 亏损 Ba、Sr、Nb、Ta、P 和 Ti, 显示 I 型花岗岩及 A 型花岗岩过渡的特征。与干沟北部较老的花岗岩相比, 晚石炭世花岗岩具有较低的( $^{87}\text{Sr}/^{86}\text{Sr}$ )(0.704771~0.705451)及较高的 $\varepsilon_{\text{Nd}}(t)$  (2.14~2.51), 显示后造山阶段有较多的新的亏损地幔源区物质的加入。文章认为晚石炭世花岗岩的形成同后造山阶段幔源岩浆底侵有关, 同时其形成为该区显生宙存在地壳垂向增生提供了新的证据。

**关键词:** 干沟; 晚石炭世; 花岗岩; 幔源岩浆底侵; 地壳增生

中图分类号: P581; 585.3; 597.3 文献标志码: A 文章编号: 1000-3657(2016)05-1545-13

## Petrogenesis and geological significance of the Late Carboniferous granites from Gangou, Central Tianshan Mountains, Xinjiang

FENG Guang-ying<sup>1</sup>, YANG Jing-sui<sup>1</sup>, LIU Fei<sup>1</sup>, NIU Xiao-lu<sup>1</sup>, GAO Jian<sup>2</sup>

(1. *CARMA, Institute of Geology, Chinese Academy of Geological Sciences, Beijing 100037, China*; 2. *Kunming University of Science and Technology, Kunming 650504, Yunnan, China*)

**Abstract:** Granitoid plutons are widespread in Gangou of Central Tianshan orogen. Previous studies of the augen granite and the fine-grained granite from north Gangou revealed that their SHRIMP U-Pb dating ages were 428 Ma and 361–368 Ma, respectively. Comparatively, zircon LA-ICP-MS U-Pb dating of the south granitoid pluton in this study yielded the  $^{206}\text{Pb}/^{238}\text{U}$  age of 301±1.0 Ma. Major and trace elements show that the granites belong to high-K calc-alkaline series, and their  $\sigma=2.67-3.22$ . In addition, they are enriched in LREE, Rb, K, Th, La, Zr and Hf, and depleted in Ba, Sr, Nb, Ta, P and Ti. They show a transitional

收稿日期: 2016-03-27; 改回日期: 2016-05-17

基金项目: 中国地质调查局工作项目(DD20160023-01, DD20160022-01)、公益性行业科研专项(201511022)、国家行业专项(SinoProbe-05-02)、自然科学基金项目 NSFC(41303019)、中国地质科学院地质研究所基本科研业务(J1321)联合资助。

作者简介: 冯光英, 女, 1983年生, 博士, 助理研究员, 主要从事岩石地球化学和岩石学方面的研究工作; E-mail: fengguangying198@163.com。

features from I-type to A-type. Compared with the Silurian–Devonian granites, late–Carboniferous granites are characterized by lower  $I_{Sr}$  values (0.704771–0.705451), higher  $\epsilon_{Nd}(t)$  (2.14–2.51) and younger  $T_{DM2}$  (861–891 Ma), suggesting that more new depleted mantle–derived materials contributed to the generation of the granites during post orogen. It is therefore held that the petrogenesis of the late–Carboniferous granites was related to the underplating of the mantle–derived magmas. This study also provides new evidence for Phanerozoic vertical continental crustal growth in the Central Asian orogenic belt.

**Key words:** Gangou; late Carboniferous; granites; mantle–derived magma underplating; crustal growth

**About the first author:** FENG Guang–ying, female, born in 1983, assistant researcher, majors in geochemistry and petrology; E–mail: fengguangying198@163.com.

**Fund support:** Supported by China Geological Survey (No. DD20160023– 01, DD20160022– 01), Ministry of Science and Technology of China (Sinoprobe–05–02, 201511022), the NSF China (No. 41303019) and the Basic Outlay of Scientific Research Work from the Ministry of Science and Technology (No. J1321).

## 1 引 言

天山造山带位于中国新疆中部,分割南部的塔里木盆地和北部的准噶尔盆地,并西延至哈萨克斯坦,总长达2500 km以上<sup>[1–4]</sup>。以中天山南、北缘古生代缝合线为界可将其分为南天山、北天山和中天山板块<sup>[5–6]</sup>(图1–a)。伊犁–中天山板块位于天山造山带的核部,西宽东窄,在库米什以东、干沟附近逐渐

变细–尖灭。一般认为,伊犁–中天山板块南北两侧的洋盆均向其下俯冲<sup>[7–8]</sup>,致使其中发育大量的侵入岩和火山岩。中天山北缘边界断裂带主要沿干沟、米什沟、乌苏通沟、冰达坂呈东西向展布,董云鹏等<sup>[9]</sup>在中天山干沟–乌苏通区段的构造混杂岩中厘定出MORB型蛇绿岩及与俯冲相关的火山岩,为中天山北缘古洋盆的存在及其俯冲削减作用提供了直接证据。对于天山造山带中出露的多条缝合

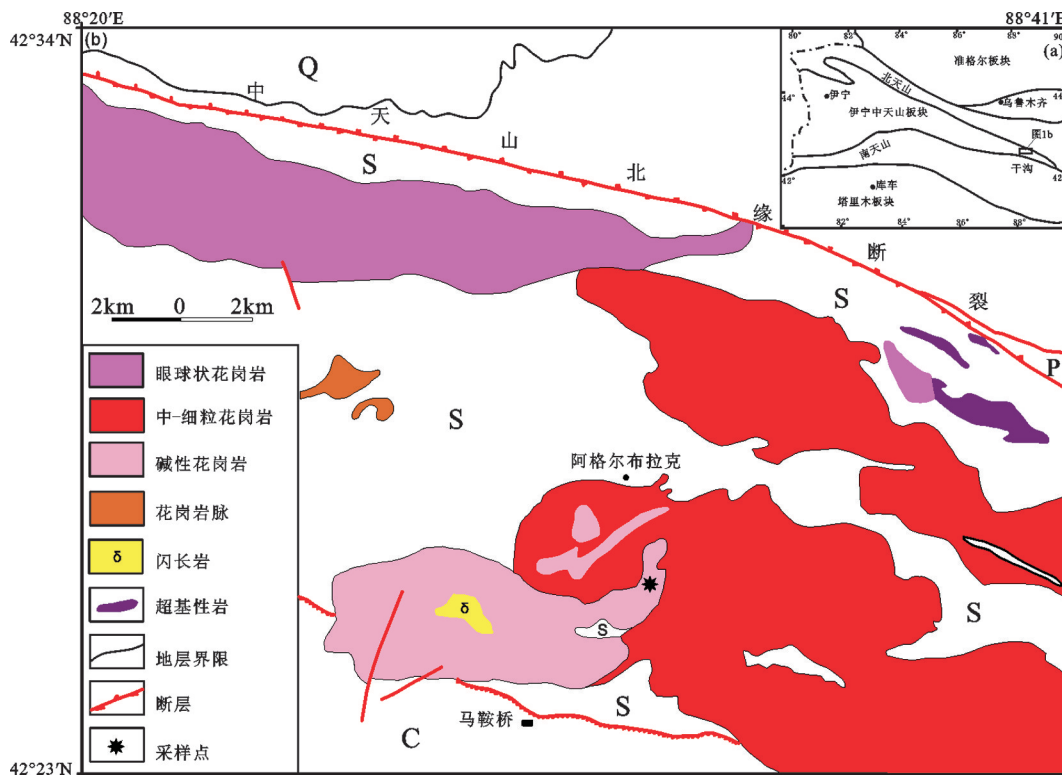


图1 天山造山带及邻区构造简图(a, 据文献[1])及干沟一带地质略图(b, 据文献[16])

Fig.1 Tectonic division of the Tianshan Orogen (a, after reference [1]) and geological sketch map of the Gangou area in the Tianshan, Xinjiang (b, after reference [16])

带<sup>[10]</sup>,其时限虽然还存在分歧,但基于该区出露的多条蛇绿岩,前人进行了大量的研究,已厘定出基本的框架。本文讨论的中天山北缘缝合带被认为是早古生代缝合带<sup>[6]</sup>,其时代为志留纪—泥盆纪,代表中天山古陆与北天山之间的缝合带<sup>[9,11]</sup>,但关于中天山北缘洋盆发展演化的过程及随后的弧—陆碰撞造山作用的时限的确定,还存在很大分歧。特别是关于中天山北缘洋盆存在及闭合的时限问题,目前主要存在2种观点,一种观点认为闭合的时间为志留纪<sup>[9,12-16]</sup>,而另一种观点则认为发生在晚石炭世—早二叠世<sup>[7-8,17]</sup>。干沟地区花岗岩广泛发育,其形成时代和地球化学性质对于深入认识造山带演化,以及后造山陆壳生长具有重要意义,石玉若等<sup>[16]</sup>对干沟北部变形强烈的眼球状花岗岩和无明显变形的细粒花岗岩进行了精确的 SHRIMP 定年研究,两者的侵位年龄分别为 428 Ma 左右和 361~368 Ma,前者代表米什沟—干沟洋盆的闭合时限,后者为碰撞造山阶段中—晚期增厚下地壳熔融的产物。本文选取该区南部研究程度较弱,没有进行精确年代学研究的高钾钙碱性花岗岩作为研究对象,并对其进行了详细的年代学及地球化学分析,对于深入探讨中天山北缘构造演化及构建该区构造演化的时间格架具有重要意义。

## 2 地质概况

中天山地块沿东经 88°大致分为东、西两段<sup>[2]</sup>,干沟位于新疆中天山东段,托克逊南,该段天山由北而南由小热泉子石炭纪褶皱带、博罗科努加里东带、巴伦台带、萨阿尔明带 4 个构造带组成,其间以断裂为界<sup>[18]</sup>。干沟早古生代蛇绿混杂岩带位于阿其克库都克断裂带以南,主要由属于弧前火山—沉积岩系的混杂基质及其裹挟的构造岩块组成,后者主要包括蛇绿岩残块,以及大理岩、花岗岩等外来构造岩块<sup>[9]</sup>。干沟蛇绿混杂岩带向西可能与米什沟蛇绿岩相连<sup>[12,14]</sup>。干沟地区花岗岩类发育<sup>[18]</sup>,与志留系呈侵入接触关系(图 1-b),这些花岗岩以前大多被认为形成于华力西期,属晚古生代的岛弧环境<sup>[16]</sup>。近年来通过高精度锆石 U—Pb 定年发现其形成年龄大多存在较大误差,有必要对其重新定年。笔者对本区南部出露的花岗岩(采样点: 42°25′48.84″N, 88°31′45.33″E)进行了精确的 LA—ICP—MS 锆石 U—

Pb 定年,确定其年龄为(301.2±1.0) Ma,即侵位于晚石炭世。

晚石炭世花岗岩整体新鲜,肉红色,中粗粒结构。同时可见多条辉绿岩脉侵入花岗岩体中,前者走向 253°,宽约 1~2.5 m 不等,风化面灰绿色,新鲜面深绿色,与花岗岩接触部位可见明显的冷凝边。

## 3 岩相学特征

干沟晚石炭世花岗岩岩体内部少见包体残留,且矿物组合未发育有定向性结构。主要矿物组成为钾长石(20%~25%)和斜长石(10%~15%)、石英(30%~50%)、少量角闪石及黑云母,副矿物主要为榍石、锆石、磁铁矿等(图 2),镜下显示长石不同程度绢云母化,黑云母绿泥石化,且绿泥石有沿着裂隙呈带状分布的特征。

## 4 分析方法

主微量元素分析在国家地质实验测试中心完成,其中主量元素采用 X 射线荧光光谱法(XRF)测定(型号: PE300D),并采用等离子光谱和化学法测定进行互检。微量元素和稀土元素采用等离子质谱法(ICP—MS)测定(型号: PW4400),同时分析 2 个国家标样(GSR3 和 GSR5)和 3 个平行样以保证分析结果的准确度。

锆石分选在河北省地矿局廊坊区调队实验室完成,采用常规粉碎、浮选和电磁选方法进行分选。锆石阴极发光(CL)照相在北京锆年领航科技有限公司电子探针实验室采用扫描电镜完成,加速电压为 15 kV。锆石原位 U—Pb 同位素年龄测定在中国地质调查局天津地质调查中心完成,仪器为 Finnigan Neptune 型 MC—ICP—MS 及与之配套的 New wave UP 193 激光剥蚀系统,激光剥蚀斑束直径为 35 μm,剥蚀深度为 20~40 μm,锆石年龄计算采用国际标准锆石 91500 作为外标,元素含量采用人工合成硅酸盐玻璃 NIST SRM610 作为外标,<sup>29</sup>Si 作为标元素进行校正。数据处理采用 ICPMSDataCal 4.3 程序,并采用软件对测试数据进行普通铅校正<sup>[19]</sup>,年龄计算及谐和图绘制采用 ISOPLOT(3.0 版)<sup>[20]</sup>软件完成。

Sr—Nd 同位素分析在南京大学现代分析中心由英国制造的 VG354 多接收质谱仪上完成,实验测定

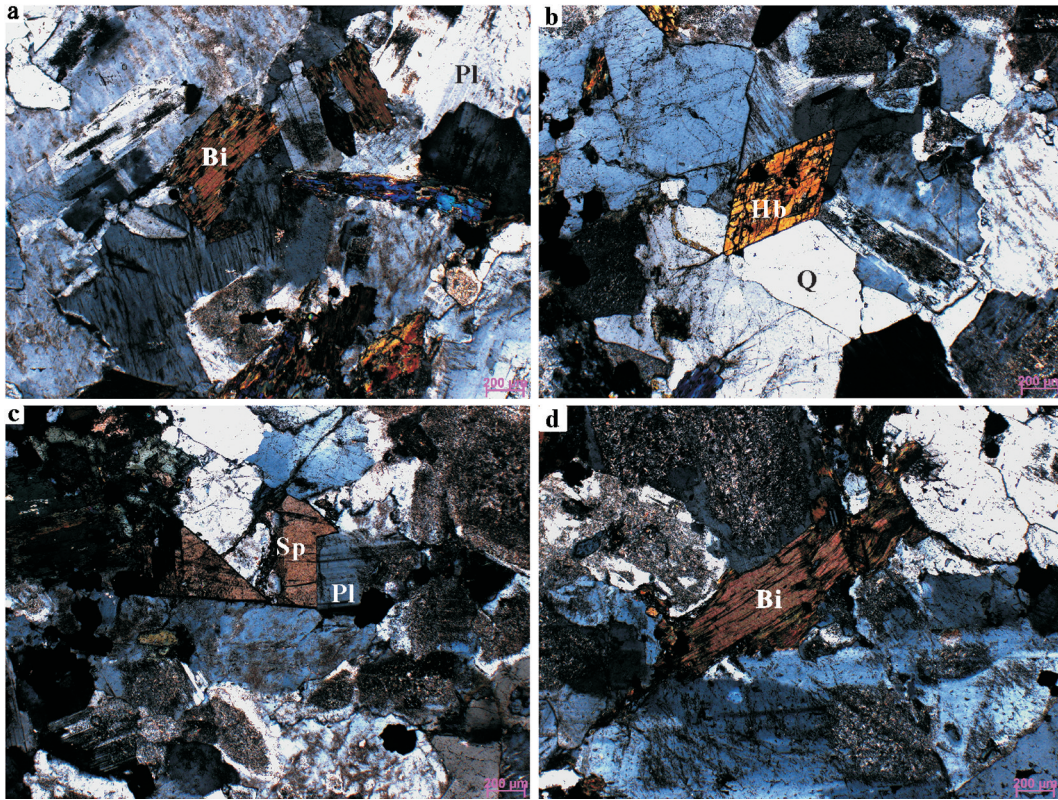


图2 干沟晚石炭世花岗岩显微镜下特征

Hb—角闪石; Bi—黑云母; Q—石英; Pl—斜长石; Sp—榍石

Fig.2 Photomicrographs of the late-Carboniferous granites in Gangou

Hb—Hornblende; Bi—Biotite; Q—Quartz; Pl—Plagioclase; Sp—Sphene

美国NBS987Sr同位素标准:以 $^{86}\text{Sr}/^{87}\text{Sr}=0.1194$ 为标准化值,测得 $^{86}\text{Sr}/^{87}\text{Sr}=0.710224\pm 8(n=10)$ ,对美国La Jolla Nd同位素标准样中 $^{143}\text{Nd}/^{144}\text{Nd}$ 的测定值为 $0.511860(2\sigma, n=8)$ ,标准化值采用 $^{143}\text{Nd}/^{144}\text{Nd}=0.7219$ 校正<sup>[21]</sup>。详细的Rb—Sr、Sm—Nd化学制备,质谱测定方法以及各类标准样品测定结果见<sup>[22]</sup>。

## 5 分析结果

### 5.1 锆石U—Pb定年

花岗岩锆石U—Pb年龄数据见表1。锆石呈自形无色透明状,锆石直径大多大于100 μm,阴极发光下都具有清晰的振荡环带,所测试锆石Th/U比值均大于0.1(0.54~1.62)(表1),具有岩浆锆石的特征。27个分析点均位于U—Pb谐和线上, $^{206}\text{Pb}/^{238}\text{U}$ 加权平均年龄为 $(301.2\pm 1.0)$  Ma(图3),代表了该岩体的结晶年龄,表明其为晚石炭世岩浆活动的产物。

### 5.2 岩石地球化学特征

花岗岩主微量元素分析结果见表2。干沟晚石

炭世花岗岩 $\text{SiO}_2$ 含量为68.48%~70.60%,碱含量较高( $\text{Na}_2\text{O} + \text{K}_2\text{O}=8.58\% \sim 9.06\%$ ), $\text{Al}_2\text{O}_3$ (14.69%~15.21%)高于一般的碱性花岗岩(一般低于12%)<sup>[23]</sup>。铝饱和指数( $A/\text{CNK}=\text{Al}_2\text{O}_3/(\text{CaO} + \text{Na}_2\text{O} + \text{K}_2\text{O})$ 克分子比值)集中于0.97~1.00,为准铝质(图4-a)。里特曼指数( $\sigma$ )为2.67~3.22,显示碱性与钙碱性过渡特点,在 $\text{SiO}_2$ — $\text{K}_2\text{O}$ 图解(图4-b)中显示高钾钙碱性花岗岩特征。

该岩石稀土元素总量较高, $\Sigma\text{REE}=141.9\times 10^{-6} \sim 193.3\times 10^{-6}$ ,稀土配分模式(图5-a)显示轻稀土明显富集的右倾型,轻重稀土分异明显, $\text{La}_N/\text{Yb}_N=11.0 \sim 16.8$ ,铕负异常( $\delta\text{Eu}=0.71 \sim 0.91$ )。在原始地幔标准化图解中(图5-b),花岗岩具有不同程度的Rb、K、Th、La、Zr及Hf富集,和Ba、Sr、Nb、Ta、P和Ti亏损,这些特征不同于I、S和M型花岗岩,而更像A型花岗岩。在A型花岗岩判别图解(图6)中,样品均位于I、S型和A型花岗岩边界附近,这些特点显示了I、S型和A型花岗岩的过渡特点。

表1 干沟托克逊晚石炭世花岗岩锆石 LA-ICP-MS U-Pb 年龄  
Table 1 Zircon U-Pb age of the Gangou late-Carboniferous granites

12YX1-15 点号	Th/ $10^{-6}$	U/ $10^{-6}$	Pb/ $10^{-6}$	Th/U	同位素比值						表面年龄 /Ma			
					$^{207}\text{Pb}/^{206}\text{Pb}$	1 $\sigma$	$^{207}\text{Pb}/^{235}\text{U}$	1 $\sigma$	$^{206}\text{Pb}/^{238}\text{U}$	1 $\sigma$	$^{207}\text{Pb}/^{235}\text{U}$	1 $\sigma$	$^{206}\text{Pb}/^{238}\text{U}$	1 $\sigma$
1	651	779	43.9	0.84	0.0511	0.0004	0.3416	0.0079	0.0485	0.0004	298	7	305	2
2	423	625	33.8	0.68	0.0523	0.0006	0.3469	0.0087	0.0481	0.0004	302	8	303	3
3	94.1	136	8.19	0.69	0.0538	0.0028	0.3570	0.0231	0.0481	0.0006	310	20	303	4
4	224	300	16.9	0.75	0.0528	0.0037	0.3507	0.0514	0.0481	0.0007	305	45	303	4
5	205	232	13.0	0.88	0.0521	0.0015	0.3427	0.0125	0.0477	0.0004	299	11	300	2
6	97.0	200	10.1	0.48	0.0511	0.0015	0.3396	0.0125	0.0482	0.0004	297	11	304	2
7	260	409	21.2	0.64	0.0527	0.0008	0.3426	0.0089	0.0472	0.0004	299	8	297	2
8	220	405	20.6	0.54	0.0539	0.0009	0.3501	0.0094	0.0471	0.0004	305	8	297	2
9	83.9	114	6.34	0.74	0.0560	0.0031	0.3690	0.0225	0.0478	0.0005	319	19	301	3
10	677	419	29.8	1.62	0.0553	0.0025	0.3633	0.0237	0.0476	0.0007	315	20	300	4
11	741	824	44.6	0.90	0.0520	0.0006	0.3429	0.0080	0.0479	0.0003	299	7	301	2
13	463	862	43.0	0.54	0.0525	0.0005	0.3454	0.0078	0.0477	0.0003	301	7	301	2
14	762	744	42.9	1.03	0.0553	0.0006	0.3637	0.0085	0.0477	0.0004	315	7	300	2
15	94.4	96.6	5.28	0.98	0.0527	0.0039	0.3475	0.0273	0.0479	0.0004	303	24	301	3
16	188	240	12.3	0.78	0.0540	0.0017	0.3492	0.0129	0.0469	0.0004	304	11	295	2
17	426	416	23.0	1.02	0.0498	0.0014	0.3353	0.0120	0.0489	0.0004	294	11	308	2
18	156	123	7.03	1.27	0.0530	0.0023	0.3500	0.0168	0.0479	0.0004	305	15	301	2
19	342	334	19.4	1.02	0.0574	0.0012	0.3771	0.0100	0.0477	0.0006	325	9	300	4
21	139	106	6.33	1.31	0.0528	0.0031	0.3493	0.0222	0.0480	0.0006	304	19	302	4
23	100	101	5.68	0.99	0.0521	0.0029	0.3431	0.0200	0.0477	0.0005	300	17	301	3
24	75.5	86.2	4.79	0.88	0.0527	0.0035	0.3465	0.0242	0.0477	0.0004	302	21	300	3
25	176	305	16.4	0.58	0.0532	0.0017	0.3520	0.0140	0.0479	0.0004	306	12	302	3
26	210	313	16.6	0.67	0.0531	0.0011	0.3497	0.0104	0.0477	0.0004	305	9	301	3
27	205	259	14.1	0.79	0.0516	0.0016	0.3414	0.0135	0.0480	0.0005	298	12	302	3
28	281	370	19.8	0.76	0.0527	0.0009	0.3482	0.0096	0.0479	0.0004	303	8	302	2
29	328	575	29.5	0.57	0.0525	0.0010	0.3456	0.0126	0.0477	0.0005	301	11	300	3
30	531	663	35.5	0.80	0.0526	0.0006	0.3460	0.0085	0.0477	0.0004	302	7	301	2

干沟晚石炭世花岗岩 Sr-Nd 同位素分析结果见表3。样品的 Sr 同位素初始比值变化于 0.70477~0.70545, Nd 同位素初始比值为 0.512360~0.512379,  $\epsilon_{\text{Nd}}(t)$  大于 0, 为 2.14~2.51。二阶段模式年龄  $T_{\text{DM2}}$  为 861~891 Ma。

## 6 讨论

### 6.1 岩石属性及构造背景

研究区花岗岩具有 I、S 型和 A 型花岗岩过渡的特征(图6)。但其铝饱和指数(A/CNK) $<1.1$ , 且岩石薄片中没有发现石榴子石、白云母或堇青石等富铝矿物, 因此不具备 S 型花岗岩的特征<sup>[28]</sup>。其  $\delta$  值为 2.67~3.22, 显示钙碱性到碱性的过渡, 属于高钾钙碱性系列的准铝质岩浆岩, 具有后碰撞花岗岩的主

要特征<sup>[29]</sup>。通常, A 型花岗岩侵位晚于 I 型花岗岩, 相对富集高场强元素, 如 Zr、Nb、Y、REE 和 Ga<sup>[30]</sup>, 而 Ca、Sr、Ba 等含量较低。干沟晚石炭世花岗岩富集 Zr 亏损 Ba、Sr, 显示 A 型花岗岩的特征, 但其亏损 Nb 和 Ta, 又显示为 I 型花岗岩的特征。通常, 高分异的 I 型花岗岩的某些特征与 A 型花岗岩颇为相似, 通过主微量元素判别图解难以有效的划分。同时, 干沟晚石炭世花岗岩中发现大量绿泥石, 且沿裂隙呈带状分布, 表明花岗岩在岩浆演化晚期受到流体作用的改造, 也使得其地球化学特征变得复杂<sup>[31]</sup>。实际上, A 型花岗岩的本质特征在于它是一种高温花岗岩, 通过锆石饱和温度计获得的 A 型花岗岩平均结晶温度通常可以达到 800°C 以上<sup>[32]</sup>。研究区花岗岩的锆石饱和温度在 882~900°C, 从这个

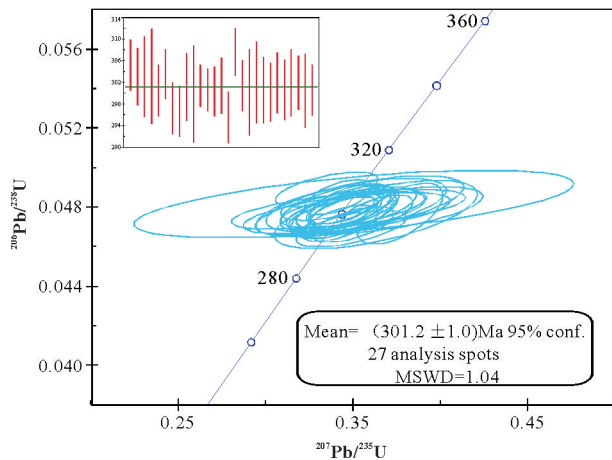


图3 干沟晚石炭世花岗岩代表性锆石的LA-ICP-MS U-Pb 谱和年龄  
Fig.3 LA-ICP-MS U-Pb age for the zircon grains from the Gangou late-Carboniferous granites

角度考虑,其形成条件更接近A型花岗岩,即此时中天山北部已处于碰撞造山后的伸展拉张阶段。此外,在微量元素Nb-Y和Rb-(Y+Nb)图解中(图7),样品主要落在火山弧花岗岩和后碰撞花岗岩重叠区域内,与Pearce et al.<sup>[33]</sup>对一些已知后碰撞花岗岩投图结果相似。前人对整个天山石炭纪火成岩进行了大量的研究,东天山博格达地区早-中石炭世双峰式火山岩系的研究表明,博格达地区在石炭纪时已经处于大陆裂谷地质构造环境<sup>[34-36]</sup>;东天山吐哈盆地南缘至喀拉塔格-星星峡地块石炭纪-

二叠纪花岗质侵入岩同样为后碰撞构造演化阶段岩浆活动的产物,主要由幔源岩浆底侵引起的地壳物质部分熔融所形成<sup>[34]</sup>;中天山中段南缘库米什地区蛇绿岩研究表明,泥盆纪期间南天山洋盆关闭,发生陆-陆碰撞和走滑作用,而该区石炭-二叠纪花岗岩形成于后碰撞构造环境<sup>[3,38]</sup>;西天山伊犁石炭-二叠纪花岗岩亦形成于后碰撞构造环境<sup>[39]</sup>;此外,朱永峰等<sup>[40]</sup>研究认为西天山晚泥盆-早石炭世岛弧自西向东逐渐消亡,取而代之的是晚石炭世碰撞后富钾岩浆的喷发。以上种种都表明,整个天山造山带在晚石炭世都已进入造山后裂谷拉伸阶段。

### 6.2 岩石成因及地壳增生

干沟晚石炭世花岗岩具有较低的Mg<sup>#</sup>(37~39),显示岩浆经历了较高级别的结晶分异作用,SiO<sub>2</sub>与TiO<sub>2</sub>和P<sub>2</sub>O<sub>5</sub>之间的负相关关系,以及微量元素蛛网图中Ti和P的亏损表明岩浆在上升过程中经历了磷灰石及榍石、角闪石、黑云母等矿物的分离结晶<sup>[37]</sup>,而Sr亏损以及负Eu异常则显示斜长石的分离结晶作用。其Nb/Ta比值为7.11~11.68,低于幔源岩石(17.5±2.0)<sup>[41-42]</sup>,而与陆壳岩石(11±)相近<sup>[42-43]</sup>,指示源区有陆壳物质的参与;同时其Zr/Hf比值为37.9~41.6,明显高于壳源岩石(约为33),而与幔源岩石(36.3±2.0)较为接近<sup>[42-43]</sup>,指示源区可能有地幔物质的参与。此外,干沟地区花岗岩Sr-Nd同位素特征亦显示晚石炭世花岗岩的形成有地幔物质的参与,干沟晚志留世(428 Ma)及中-晚泥盆世(360~368 Ma)花岗岩具有较高的(<sup>87</sup>Sr/<sup>86</sup>Sr)比值(0.70689~

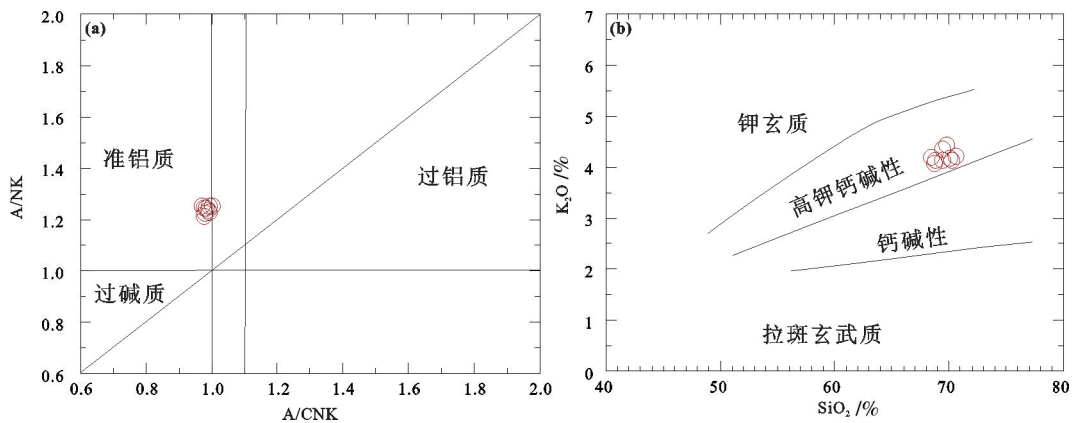


图4 干沟晚石炭世花岗岩主要元素的岩石类型图解  
Fig.4 Major element diagrams for rock types of the late-Carboniferous granites from Gangou

表2 干沟晚石炭世花岗岩的主量元素(%)及微量元素( $10^{-6}$ )分析结果

Table 2 Major (%) and trace elements ( $10^{-6}$ ) compositions of the Gangou late-Carboniferous granites									
分析项目	12YX1-6	12YX1-7	12YX1-8	12YX1-9	12YX1-10	12YX1-13	12YX1-14	12YX1-16	12YX1-17
SiO <sub>2</sub>	69.47	69.46	70.60	68.48	69.79	68.78	70.28	68.76	70.07
Al <sub>2</sub> O <sub>3</sub>	14.99	15.17	14.69	15.21	15.00	15.00	14.75	15.13	14.78
CaO	1.72	1.77	1.59	1.66	1.64	1.68	1.77	1.92	1.55
TFe <sub>2</sub> O <sub>3</sub>	2.83	2.72	2.70	2.93	2.50	3.01	2.69	2.85	2.76
K <sub>2</sub> O	4.14	4.35	4.21	4.20	4.43	4.13	4.13	4.07	4.18
MgO	0.80	0.78	0.75	0.77	0.68	0.87	0.74	0.81	0.76
MnO	0.06	0.05	0.05	0.05	0.05	0.07	0.06	0.07	0.07
Na <sub>2</sub> O	4.56	4.56	4.37	4.86	4.47	4.73	4.49	4.68	4.58
P <sub>2</sub> O <sub>5</sub>	0.17	0.15	0.15	0.17	0.14	0.17	0.14	0.17	0.15
TiO <sub>2</sub>	0.47	0.45	0.45	0.49	0.41	0.50	0.45	0.47	0.46
LOI	0.83	0.51	0.72	1.27	0.65	1.00	0.54	0.54	0.90
Total	100.04	99.97	100.28	100.09	99.76	99.94	100.04	99.47	100.26
Na <sub>2</sub> O+K <sub>2</sub> O	8.70	8.91	8.58	9.06	8.90	8.86	8.62	8.75	8.76
A/CNK	0.99	0.98	1.00	0.98	0.99	0.98	0.98	0.97	0.99
A/NK	1.25	1.24	1.25	1.21	1.23	1.22	1.24	1.25	1.22
$\delta$	2.86	3.00	2.67	3.22	2.96	3.04	2.72	2.97	2.83
Mg <sup>#</sup>	38	39	38	37	37	39	38	38	38
Cr	3.24	13.30	2.98	4.58	2.90	9.79	2.70	2.70	3.56
Mn	489	358	349	369	406	521	465	575	509
Co	3.84	3.68	3.69	3.87	3.45	4.33	3.69	3.88	3.94
Ni	3.01	7.66	2.66	4.15	2.56	8.21	2.84	2.86	3.04
Cu	8.44	7.28	14.90	8.87	4.77	8.29	4.37	4.59	4.84
Zn	29.9	68.1	30.4	30.8	31.1	35.1	34.2	39.8	37.7
Ga	17.6	17.0	17.8	18.7	17.5	17.9	17.5	18.4	17.8
Rb	90.70	93.70	97.30	107	108	91.10	105	114	109
Sr	312	310	296	293	313	298	293	324	281
Ba	729	769	690	676	742	749	668	679	702
Pb	16.4	15.4	17.1	11.6	17.5	15.7	15.9	16.5	17.3
Th	12.1	15.4	11.7	12.6	11.1	12.7	13.2	13.4	21.0
U	2.92	2.24	2.21	2.14	1.91	3.14	1.73	1.86	2.48
Nb	14.7	13.7	13.9	15.7	13.2	15.5	14.5	16.9	15.5
Ta	1.31	1.23	1.32	1.45	1.13	1.55	1.33	1.70	2.18
Zr	336	312	321	313	281	289	288	296	324
Hf	8.69	8.00	8.12	8.01	6.76	7.62	7.44	7.63	8.48
Ti	2792	2575	2655	2898	2427	2928	2632	2806	2661
V	25.2	23.1	24.5	27.2	22.4	25.8	23.1	25.6	23.6
Y	17.7	16.6	17.3	20.4	15.5	19.2	17.7	20.8	19.9
La	40.1	39.5	39.3	34.0	33.5	34.4	47.6	45.7	47.5
Ce	73.6	70.0	76.0	66.2	61.7	65.8	83.3	82.2	82.4
Pr	8.45	8.06	8.17	7.23	6.72	7.65	9.27	9.37	9.54
Nd	31.2	29.0	30.1	27.6	24.4	29.0	33.8	33.7	33.4
Sm	4.71	4.44	4.41	4.74	3.79	4.86	4.84	5.07	5.01
Eu	1.18	1.14	1.12	1.19	1.07	1.13	1.11	1.14	1.14
Gd	4.00	3.62	3.61	4.05	3.27	4.16	4.07	4.63	4.20
Tb	0.56	0.54	0.54	0.64	0.47	0.62	0.57	0.65	0.64
Dy	3.21	3.02	3.06	3.57	2.71	3.56	3.13	3.59	3.52
Ho	0.63	0.60	0.59	0.71	0.52	0.70	0.64	0.70	0.70
Er	1.90	1.77	1.82	2.13	1.62	2.10	1.89	2.20	2.15
Tm	0.29	0.27	0.28	0.32	0.24	0.30	0.28	0.31	0.33
Yb	2.07	1.93	1.91	2.22	1.66	2.23	2.03	2.35	2.35
Lu	0.32	0.31	0.31	0.35	0.27	0.33	0.33	0.37	0.37
$\Sigma$ REE	172.2	164.2	171.2	155.0	141.9	156.8	192.9	192.0	193.3
La <sub>N</sub> /Yb <sub>N</sub>	13.9	14.7	14.8	11.0	14.5	11.1	16.8	13.9	14.5
$\delta$ Eu	0.81	0.84	0.83	0.81	0.91	0.75	0.74	0.71	0.74
T <sub>Zr</sub> <sup>100</sup> C	900	892	898	891	882	883	884	885	897

0.70981), 以及负的  $\epsilon_{Nd}(t)$  值 (-5.3~ -1.6), 模式年龄较老 (1.21~1.50 Ga)<sup>[6]</sup>, 它们的  $\epsilon_{Nd}(t)$  值比较接近古一中元古代陆壳, 其物源主要为古老的地壳物质, 与此相反, 干沟晚石炭世花岗岩具有较低的 ( $^{87}\text{Sr}/^{86}\text{Sr}$ )<sub>i</sub> 比值 (0.704771~0.705451), 以及正的  $\epsilon_{Nd}(t)$  值 (2.14~2.51), 且二阶段模式年龄较为年轻 (图 8),  $T_{DM2}$  为 861~891 Ma。这种 Sr-Nd 同位素特征在整个中亚造山带晚古生代—中生代期间普遍存在<sup>[44-49]</sup>, 显示随着时间的推移, 有新的亏损地幔源区物质的加入。

中亚造山带是世界上最大的增生造山带之一,

且持续时间较长<sup>[50-52]</sup>。同造山正  $\epsilon_{Nd}(t)$  花岗岩最可能与洋壳俯冲有关, 指示陆壳水平增生, 而后造山正  $\epsilon_{Nd}(t)$  花岗岩可能指示新幔源物质加入导致的地壳垂向生长, 也可以是已增生的年轻地壳 (包括洋壳) 再循环的产物<sup>[23, 53-55]</sup>, 指示水平增生; 还可以是前造山 (新元古代) 底侵的基性下地壳再熔产物 (如吴福元等<sup>[56]</sup>), 反映了元古宙垂向增生<sup>[44]</sup>。后造山阶段壳幔相互作用为主, 花岗岩中的年轻物质最有可能与新的幔源岩浆底侵有关<sup>[44]</sup>。东天山地区晚石炭世晚期—二叠纪除发育大量花岗岩之外, 还发育基性、

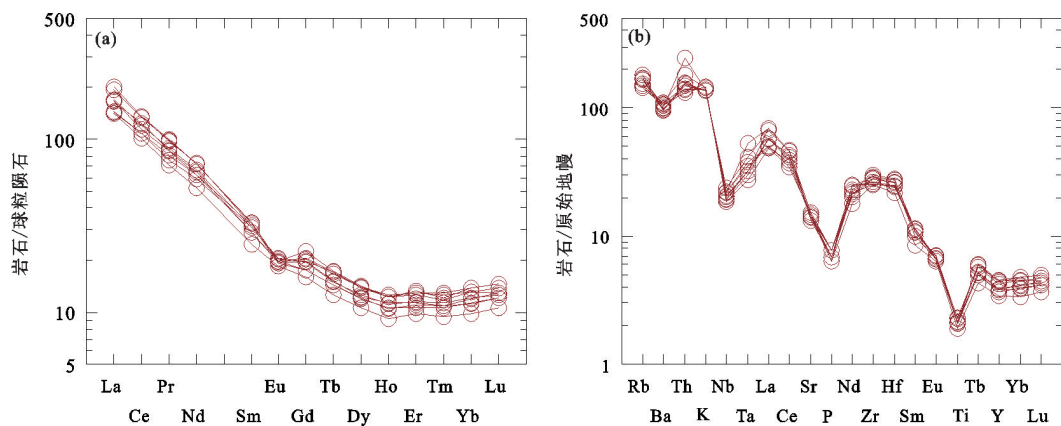


图5 干沟晚石炭世花岗岩岩体的稀土元素球粒陨石标准化图解(a)及原始地幔标准化蛛网图(b)<sup>[24]</sup>  
Fig.5 Chondrite-normalized REE distribution pattern (a) and primitive mantle normalized spidergram (b) for the late-Carboniferous granites from Gangou (after reference [24])

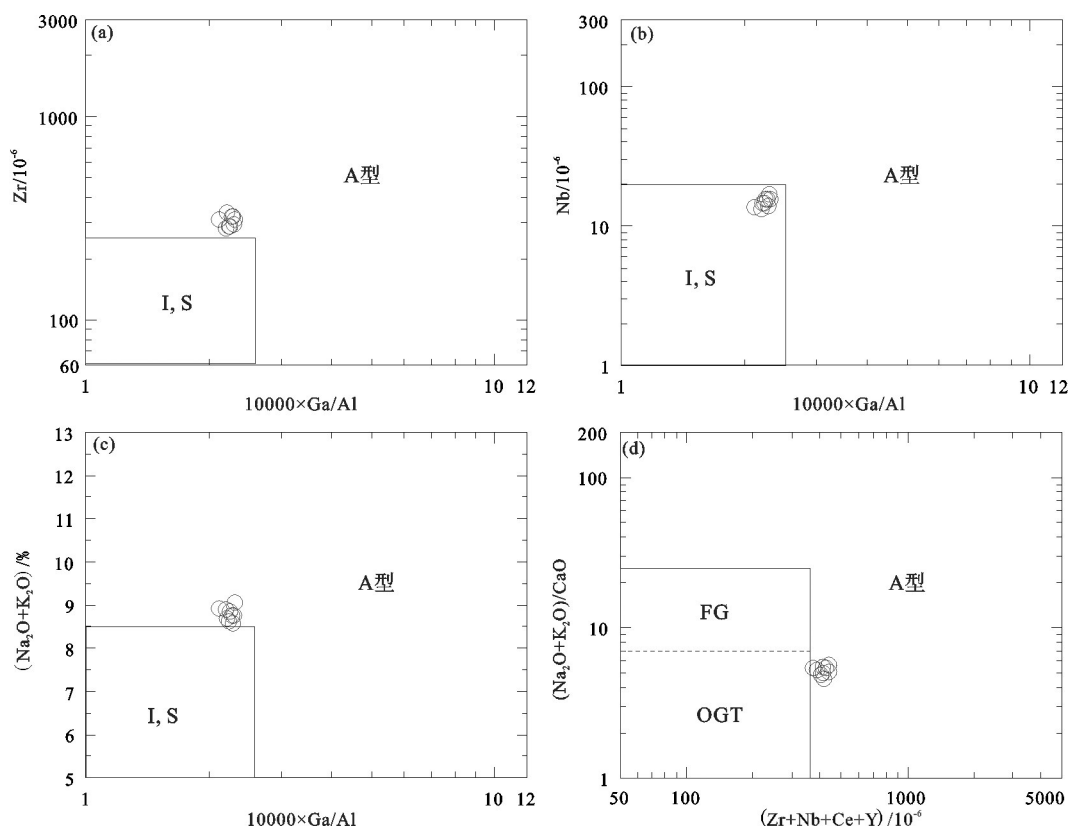


图6 干沟晚石炭世花岗岩在A型花岗岩判别图解中的位置(据参考文献[25])

I, S—I型和S型花岗岩分布区; FG—分异的I, S型花岗岩分布区; OGT—I, S, M型花岗岩分布区

Fig.6 Locations of the the Gangou late-Carboniferous granites in discrimination diagrams for A-type granites (after reference[25])

I, S—Field for I- and S-type granitoids, FG—Field for fractioned I- and S-type granitoids, OGT—Field for I-, S-, and M-type granitoids



表3 干沟晚石炭世花岗岩 Rb-Sr 和 Sm-Nd 同位素组成  
Table 3 Rb-Sr and Sm-Nd isotopic composition of the late-Carboniferous granitoids from Gangou

样号	Rb/10 <sup>-6</sup>	Sr/10 <sup>-6</sup>	<sup>87</sup> Rb/ <sup>86</sup> Sr	<sup>87</sup> Sr/ <sup>86</sup> Sr	±2σ	( <sup>87</sup> Sr/ <sup>86</sup> Sr) <sub>i</sub>	Sm/10 <sup>-6</sup>	Nd/10 <sup>-6</sup>	<sup>147</sup> Sm/ <sup>144</sup> Nd	<sup>143</sup> Nd/ <sup>144</sup> Nd	±2σ	( <sup>143</sup> Nd/ <sup>144</sup> Nd) <sub>i</sub>	ε <sub>Nd</sub> (t)	T <sub>DM2</sub> /Ma
12YX1-6	88.26	308.4	0.8453	0.709072	7	0.70545	4.816	32.46	0.0894	0.512536	7	0.512360	2.14	891
12YX1-7	94.51	317.9	0.8796	0.709125	8	0.70536	4.527	30.14	0.0909	0.512547	9	0.512368	2.30	879
12YX1-8	98.2	305.2	0.9485	0.709383	8	0.70532	4.36	28.97	0.0913	0.512556	8	0.512376	2.45	865
12YX1-9	105.4	290.6	1.0640	0.709328	9	0.70477	4.834	28.56	0.1027	0.512574	9	0.512372	2.37	872
12YX1-10	106.10	308.3	1.0170	0.709319	7	0.70496	4.012	26.08	0.0934	0.512563	8	0.512379	2.51	861

注:计算所用球粒陨石均一岩浆库值 (<sup>87</sup>Rb/<sup>86</sup>Sr=0.0847, <sup>87</sup>Sr/<sup>86</sup>Sr=0.7045, <sup>147</sup>Sm/<sup>144</sup>Nd=0.1967, <sup>143</sup>Nd/<sup>144</sup>Nd=0.512638), λ<sub>Rb</sub>=1.42×10<sup>-11</sup> a<sup>-1</sup> (据文献[26]); λ<sub>Sm</sub>=6.54×10<sup>-12</sup> a<sup>-1</sup> (据文献[27])。

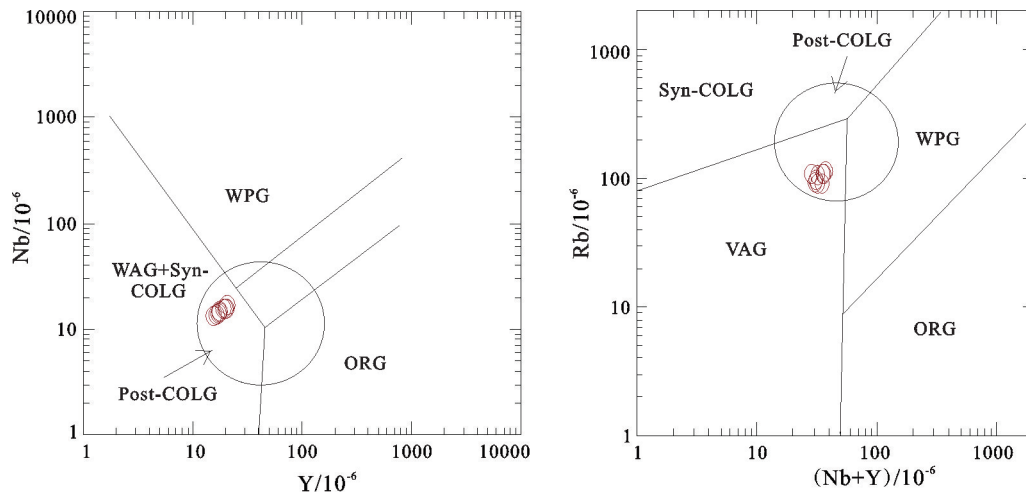


图7 花岗岩微量元素构造环境判别图(据文献[30])

VAG—火山弧花岗岩; WPG—板内花岗岩; S-COLG—同碰撞花岗岩; ORG—洋中脊花岗岩, Post-COLG—后碰撞花岗岩

Fig. 7 Y-Nb and (Nb+Y)-Rb tectonic discrimination diagram (after reference [33])

VAG—Vocanic arc granites; WPG—Within -plate granites; S-COLG—Syncollisional granites; ORG—Ocean-ridge granites; Post-COLG—Post collisional granites

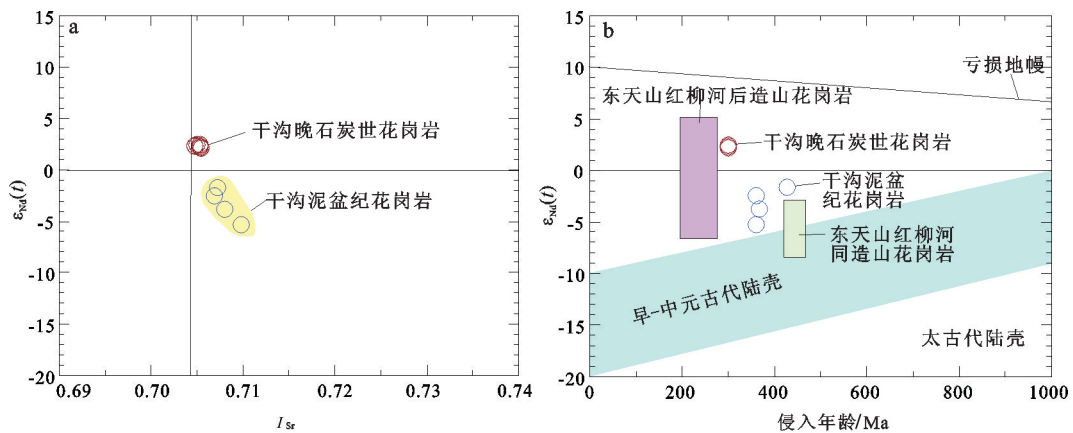


图8 干沟地区花岗岩 I<sub>Sr</sub>-ε<sub>Nd</sub>(t)图解(a)及侵入年龄-ε<sub>Nd</sub>(t)图解(b)

干沟泥盆纪花岗岩据文献[16], 东天山红柳河同造山花岗岩和后造山花岗岩据文献[44]

Fig. 8 I<sub>Sr</sub>-ε<sub>Nd</sub>(t) diagram (a) and intrusive age (Ma)-ε<sub>Nd</sub>(t) diagram (b) for the late-Carboniferous granites from Gangou, the field for Gangou Devonian granites are from reference [16], the field for syn-orogenic and post-orogenic granites from Hongliuhe, eastern Tianshan are after reference [44]

超基性杂岩以及基性岩墙<sup>[57-59]</sup>,也说明这个时期的花岗岩很可能与幔源岩浆底侵有关<sup>[37]</sup>。此外,前人的研究发现在中天山北缘阿其克库都克断裂带以南存在一个晚石炭世花岗岩带,其岩性为I型和A型花岗岩组合。其中I型花岗岩中常见大量的基性岩浆包体,也说明与I型花岗岩组合同期有幔源岩浆活动<sup>[60]</sup>。新的幔源物质的加入显示干沟晚石炭世存在地壳垂向生长。

从区域构造演化看,中天山北缘蛇绿岩形成于中寒武世—早奥陶世,亦代表了中天山北缘古洋盆存在时限,到中—晚奥陶世,该洋盆关闭,继之以南北地块的对接、碰撞,早志留世,该带转换为对接后的陆表沉积环境,堆积复理石建造<sup>[7]</sup>。到中—晚泥盆世该区处于造山下地壳增厚阶段,此后增厚下地壳将发生拆离和下沉,造成热的软流圈地幔替代、上隆,发生部分熔融,产生后造山岩浆作用,并相应诱发拉伸体制。晚石炭世中天山北缘已经处于造山后的伸展拉张阶段,后造山阶段,板块俯冲碰撞的动力学机制已经结束,幔源岩浆底侵可以为后造山岩浆活动提供新的动力学及物源<sup>[44,61]</sup>。结合研究区晚石炭世花岗岩特征,笔者认为干沟晚石炭世花岗岩为壳幔相互作用的产物,由幔源岩浆底侵引起地壳部分熔融产生的岩浆经过高度结晶分异而形成,其形成表明晚石炭世中天山北缘已处于造山后伸展阶段,同时为中亚造山带存在显生宙垂向增生提供新的依据。

## 7 结 论

(1)中天山干沟一带晚石炭世花岗岩为后造山伸展拉张阶段岩浆活动的产物,其锆石 LA-ICP-MS U-Pb 定年结果为(301±1.0) Ma。

(2)干沟晚石炭世花岗岩属于高钾钙碱性系列,其 $\sigma$ 值为2.67~3.22,显示钙碱性与碱性过渡的特点,其主微量元素显示I型花岗岩及A型花岗岩过渡的特征。同时该花岗岩体具有较低的( $^{87}\text{Sr}/^{86}\text{Sr}$ )<sub>i</sub>(0.704771~0.705451),较高的 $\epsilon_{\text{Nd}}(t)$ (2.14~2.51)及较为年轻的二阶段模式年龄( $T_{\text{DM}2}$ =861~891 Ma),其形成同后造山阶段幔源岩浆底侵有关,同时指示该区存在显生宙垂向地壳增生。

**致谢:**田亚洲博士、王云鹏硕士、赵一珏硕士在野外样品采集及实验测试过程中给予了很大帮助,

在此表示衷心感谢!

## 参考文献(References):

- [1] Gao J, Li M S, Xiao X C, et al. Paleozoic tectonic evolution of the Tianshan Orogen, northwestern China[J]. *Tectonophysics*, 1998, 287: 213-231.
- [2] Wang M, Zhang J J, Zhang B, et al. An Early Paleozoic collisional event along the northern margin of the Central Tianshan Block: Constraints from geochemistry and geochronology of granitic rocks[J]. *Journal of Asian Earth Sciences*, 2015, 113(1): 325-338.
- [3] 杨经绥,徐向珍,李天福,等.新疆中天山南缘库米什地区蛇绿岩的锆石 U-Pb 同位素定年:早古生代洋盆的证据[J]. *岩石学报*, 2011, 27(01): 77-95.  
Yang Jingsui, Xu Xiangzhen, Li Tianfu, et al. U-Pb ages of zircons from ophiolite and related rocks in the Kumishi region at the southern margin of Middle Tianshan, Xinjiang: Evidence of Early Paleozoic oceanic basin[J]. *Acta Petrologica Sinica*, 2011, 27(1): 77-95 (in Chinese with English abstract).
- [4] 林彦嵩,张泽明,贺振宇,等.中天山北缘华力西期造山作用——变质锆石 U-Pb 年代学限定[J]. *中国地质*, 2011, 38(4): 820-828.  
Lin Yanhao, Zhang Zeming, He Zhenyu, et al. Variscan orogeny of Central Tianshan Mountains: Constrains from zircon U-Pb chronology of high-grade metamorphic rocks[J]. *Geology in China*, 2011, 38(4): 820-828 (in Chinese with English abstract).
- [5] 牛晓露,杨经绥,刘飞,等.新疆中天山南缘乌瓦门地区蛇绿岩中超镁铁岩的成因:来自岩石矿物学和地球化学的证据[J]. *中国地质*, 2015, 42(5): 1404-1420.  
Niu Xiaolu, Yang Jingsui, Liu Fei, et al. Mineralogical and geochemical constraints on the origin of the ultramafic rocks from Wuwamen ophiolite on the southern margin of Middle Tianshan Mountains, Xinjiang[J]. *Geology in China*, 2015, 42(5): 1404-1420 (in Chinese with English abstract).
- [6] 肖序常,汤耀庆,冯益民,等.新疆北部及其邻区大地构造[M].北京:地质出版社,1992:1-169.  
Xiao Xuchang, Tang Yaoqin, Feng Yimin, et al. *Tectonic of Northern Xinjiang and the Adjacent Areas*[M]. Beijing: Geological Publishing House, 1992:1-169 (in Chinese with English abstract).
- [7] Windley B F, Allen B M, Zhang C, et al. Paleozoic accretion and Cenozoic reformation of the Chinese Tien Shan Range, central Asia[J]. *Geology*, 1990, 18(2): 128-131.
- [8] Allen M B, Windley B F, Zhang C. Junger, Turfan and Alakol basins as Late Permian to Early Triassic extensional structures in a sinistral shear zone in the Altaid orogenic collage, Central Asia[J]. *J. Geol. Soc. Lond*, 1992, 152: 327-338.
- [9] 董云鹏,周鼎武,张国伟,等.中天山北缘干沟蛇绿混杂岩带的地质地球化学[J]. *岩石学报*, 2006, 22(01): 49-56.  
Dong Yunpeng, Zhang Guowei, Zhou Dingwu, et al. *Geology and geochemistry of the Ganou ophiolitic mélangé at the northern margin of the Middle Tianshan Belt*[J]. *Acta Petrologica Sinica*,

- 2006, 22(01): 49–56(in Chinese with English abstract).
- [10] 赵一珏, 杨经绥, 刘仕军, 等. 新疆中天山巴仑台闪长岩成因及其地质意义[J]. 中国地质, 2015, 42(5): 1228–1241.  
Zhao Yijue, Yang Jingsui, Liu Shijun, et al. The origin of the Baluntai diorite in Central Tianshan Mountains, Xinjiang, and its geological significance[J]. *Geology in China*, 2015, 42(5): 1228–1241(in Chinese with English abstract).
- [11] 郭召杰, 张志诚. 中天山早古生代岛弧构造带研究[J]. 石家庄经济学院学报, 1993, 16(2): 132–139.  
Guo Zhaojie, Zhang Zhicheng. On the Early Paleozoic island arc belt of Mid-Tianshan[J]. *Journal of Shijiazhuang University of Economics*, 1993, 16(2): 132–139(in Chinese with English abstract).
- [12] 车自成, 刘洪福, 刘良, 等. 中天山造山带的形成与演化[M]. 北京: 地质出版社, 1994.  
Che Zicheng, Liu Hongfu, Liu Liang, et al. Formation and Evolution of the Middle Tianshan Mountain Orogenic Belt[M]. Beijing: Geological Publishing House, 1994(in Chinese with English abstract).
- [13] 舒良树, 夏飞雅克, 马瑞士. 中天山北缘大型右旋走滑切剪带研究[J]. 新疆地质, 1998, 16(4): 326–336.  
Shu Liangshu, Charvet Jacques, Ma Ruishi. Study of a large Paleozoic dextral-slip ductile shear zone along the northern margin of the central Tianshan, Xinjiang [J]. *Xinjiang Geology*, 1998, 16(4): 326–336(in Chinese with English abstract).
- [14] 朱宝清, 冯益民, 杨军录, 等. 新疆中天山干沟一带蛇绿混杂岩和志留纪前陆盆地的发现及其意义[J]. 新疆地质, 2002, 20(4): 326–330.  
Zhu Baoqing, Feng Yimin, Yang Junlu, et al. Discovery of ophiolitic mélangé and Silurian foreland basin at Gangou of Tokxun, Xinjiang and their tectonic significance[J]. *Xinjiang Geology*, 2002, 20(4): 326–330(in Chinese with English abstract).
- [15] 董云鹏, 张国伟, 周鼎武, 等. 中天山北缘冰达坂蛇绿混杂岩的厘定及其构造意义[J]. 中国科学: D辑, 2005, 35(6): 552–560.  
Dong Yunpeng, Zhang Guowei, Zhou Dingwu, et al. Geology and geochemistry of the Bingdaban ophiolitic mélangé in the boundary fault zone on the northern Central Tianshan Belt, and its tectonic implications[J]. *Science in China(Ser. D)*, 2005, 35(6): 552–560 (in Chinese).
- [16] 石玉若, 刘敦一, 张旗, 等. 中天山干沟一带花岗质岩类 SHRIMP 年代学及其构造意义[J]. 科学通报, 2006, 51(22): 2665–2672.  
Shi Yuruo, Liu Dunyi, Zhang Qi, et al. SHRIMP zircon U–Pb dating of the Gangou granitoids, Central Tianshan Mountains, Northwest China and tectonic significances[J]. *Chinese Science Bulletin*, 2006, 51(22): 2665–2672(in Chinese).
- [17] Xiao W J, Zhang L C, Qin K Z, et al. Paleozoic accretionary and collisional tectonic of the Eastern Tianshan (China): implications for the continental growth of central Asia[J]. *American Journal of Science*, 2004, 304: 370–395.
- [18] 周汝洪, 刘正荣, 裴江平, 等. 新疆天山干沟加里东花岗岩构造环境[J]. 新疆地质, 2009, 27(4): 308–314.  
Zhou Ruhong, Liu Zhengrong, Pei Jiangping, et al. Tectonic setting of the Gangou Caledonian granite in Tianshan of Xinjiang, and its contrast with Precambrian granite in Middle Tianshan Mountain[J]. *Xinjiang Geology*, 2009, 27(4): 308–314 (in Chinese with English abstract).
- [19] Andersen T. Correction of common lead in U–Pb analyses that do not report  $^{204}\text{Pb}$ [J]. *Chem. Geol.* 2002, 192, 59–79.
- [20] Ludwig K R. ISOPLOT 3.00: A Geochronological Toolkit for Microsoft Excel[CP]. Berkeley. Geochronology Center, California, 2003.
- [21] 王银喜, 顾连兴, 张遵忠, 等. 东天山晚石炭世大石头群流纹岩 Sr–Nd–Pb 同位素地球化学研究[J]. 岩石学报, 2007, 23(7): 1749–1755.  
Wang Yinxi, Gu Lianxing, Zhang Zunzhong et al. Sr–Nd–Pb isotope geochemistry of Rhyolite of the Late Carboniferous Dashitou group in eastern Tianshan[J]. *Acta Petrological Sinica*, 2007, 23(7): 1749–1755(in Chinese with English abstract).
- [22] Wang Y X, Yang J D, Chen Jun, et al. The Sr and Nd isotopic variations of the Chinese Loess Plateau during the past 7 Ma: Implications for the East Asian winter monsoon and source areas of loess[J]. *Palaeogeography Palaeoclimatology Palaeoecology*, 2007, 249 (3–4): 351–361.
- [23] 王涛, 洪大卫, 童英, 等. 中国阿尔泰造山带后造山喇嘛昭花岗岩体锆石 SHRIMP 年龄、成因及陆壳垂向生长意义[J]. 岩石学报, 2005, 21(3): 640–650.  
Wang Tao, Hong Dawei, Tong Ying, et al. Zircon U–Pb SHRIMP age and origin of post-orogenic Lamazhao granite pluton from Altai orogen: its implications for vertical continental growth[J]. *Acta Petrologica Sinica*, 2005, 21(3): 640–650(in Chinese with English abstract).
- [24] Sun S S, McDonough W F. Chemical and isotope systematics of oceanic basalts: Implications for mantle composition and processes[C]//Saunders A Dand Norry M J ( eds. ). *Magmatism in Ocean Basins*. London: Geological Society Publication, 1989, 42: 313–345.
- [25] Whalen J B, Currie K L, Chappell B W. A-type granites: geochemical characteristics, discrimination and petrogenesis[J]. *Contrib. Mineral. Petrol.*, 1987, 95: 407–419.
- [26] Steiger R H, Jäger E. Subcommission on geochronology: convention on the use of decay constants in geochronology and cosmochronology[J]. *Earth Planetary Science Letters*, 1977, 36: 359–362.
- [27] Lugmair G W, Harti K. Lunar initial  $^{143}\text{Nd}/^{144}\text{Nd}$ : differential evolution of the lunar crust and mantle[J]. *Earth Planetary Science Letters*, 1978, 39: 349–357.
- [28] 龙灵利, 高俊, 熊贤明, 等. 新疆中天山南缘比开(地区)花岗岩地球化学特征及年代学研究[J]. 岩石学报, 2007, 23(4): 719–

732.  
Long Lingli, Gao Jun, Xiong Xianming, et al. Geochemistry and geochronology of granitoids in Bikai region, southern Central-Tianshan mountains, Xinjiang[J]. *Acta Petrologica Sinica*, 2007, 23 (4): 719-732(in Chinese with English abstract).
- [29] Liegeois J P, Naves J, Hertogen J, et al. Contrasting origin of post-collisional high-K calc-alkaline and shoshonitic versus alkaline and peralkaline granitoids[J]. *Lithos*, 1989, 5: 1-28.
- [30] Wu F Y, Jahn B M, Wilde S A, et al. Highly fractionated I-type granites in NE China (I): geochronology and petrogenesis[J]. *Lithos*, 2003, 66, 241-273.
- [31] 陈璟元, 杨进辉. 佛冈高分异I型花岗岩的成因: 来自Nb-Ta-Zr-Hf等元素的制约[J]. *岩石学报*, 2015, 31(3): 846-854.  
Chen Jingyuan, Yang Jinhui. Petrogenesis of the Fogang highly fractionated I-type granitoids: Constraints from Nb, Ta, Zr and Hf[J]. *Acta Petrologica Sinica*, 2015, 31(3): 846-854(in Chinese with English abstract).
- [32] 李小伟, 莫宣学, 赵志丹, 等. 关于A型花岗岩判别过程中若干问题的讨论[J]. *地质通报*, 2010, 29(2-3): 278-285.  
Li Xiaowei, Mo Xuanxue, Zhao Zhidan, et al. A discussion on how to discriminate A-type granite[J]. *Geological Bulletin of China*, 2010, 29(2/3):278-285(in Chinese with English abstract).
- [33] Pearce J A, Harris B W, Tindle A G. Trace element discrimination diagrams for the tectonic interpretation of granitic rocks[J]. *Journal of Petrology*, 1984, 25(4): 956-983.
- [34] 夏林圻, 张国伟, 夏祖春, 等. 天山古生代洋盆开启、闭合时限的岩石学约束——来自震旦纪、石炭纪火山岩的证据[J]. *地质通报*, 2002, 21(2):55-62.  
Xia Linqi, Zhang Guowei, Xia Zuchun, et al. Constraints on the timing of opening and closing of the Tianshan Paleozoic oceanic basin: Evidence from Sinian and Carboniferous volcanic rocks[J]. *Geological Bulletin of China*, 2002, 21(2):55-62 (in Chinese with English abstract).
- [35] 夏林圻, 夏祖春, 徐学义, 等. 天山石炭纪大火成岩省与地幔柱[J]. *地质通报*, 2004, 23 (9/10): 903-910.  
Xia Linqi, Xia Zuchun, Xu Xueyi, et al. Carboniferous Tianshan igneous megaprovince and mantle plume[J]. *Geological Bulletin of China*, 2004, 23(9/10): 903-910 (in Chinese with English abstract).
- [36] 顾连兴, 胡受奚, 于春水, 等. 东天山博格达造山带石炭纪火山岩及其形成地质环境[J]. *岩石学报*, 2000, 16 (3): 305-316.  
Gu Lianxing, Hu Shouxi, Yu Chunshui, et al. Carboniferous volcanites in the Bagda orogenic belt of eastern Tianshan: their tectonic implications[J]. *Acta Petrologica Sinica*, 2000, 16 (3): 305-316 (in Chinese with English abstract).
- [37] 董庆吉, 丛源, 肖克炎. 东天山石炭纪—二叠纪花岗质侵入岩的地球化学及地质意义[J]. *地质学刊*, 2014, 38 (4): 517-529.  
Dong Qingji, Cong Yuan, Xiao Keyan. 2014. Geochemical and geological implications of granitic intrusive rocks in Carboniferous to Permian in eastern Tianshan of Xinjiang[J]. *Journal of Geology*, 38 (4): 517-529 (in Chinese with English abstract).
- [38] 杨经绥, 徐向珍, 李天福, 等. 新疆中天山南缘库米什地区蛇绿岩的锆石U-Pb同位素定年: 早古生代洋盆的证据[J]. *岩石学报*, 2011, 27(1): 77-95.  
Yang Jingsui, Xu Xiangzhen, Li Tianfu, et al. U-Pb ages of zircons from ophiolite and related rocks in the Kumishi region at the southern margin of Middle Tianshan, Xinjiang: Evidence of Early Paleozoic oceanic basin[J]. *Acta Petrologica Sinica*, 2011, 27(1): 77-95 (in Chinese with English abstract).
- [39] 徐学义, 马中平, 夏祖春, 等. 天山中西段古生代花岗岩TIMS法锆石U-Pb同位素定年及岩石地球化学特征研究[J]. *西北地质*, 2006, 39(1): 50-75.  
Xu Xueyi, Ma Zhongping, Xia Xuchun, et al. TIMS U-Pb isotopic dating and geochemical characteristics of Paleozoic granitic rocks from the Middle-Western section of Tianshan[J]. *Northwestern Geology*, 2006, 39(1): 50-75 (in Chinese with English abstract).
- [40] 朱永峰, 周晶, 郭璇. 西天山石炭纪火山岩岩石学及Sr-Nd同位素地球化学研究[J]. *岩石学报*, 2006, 22 (5): 1341-1350.  
Zhu Yongfeng, Zhou Jing, Guo Xuan. Petrology and Sr-Nd isotopic geochemistry of the Carboniferous volcanic rocks in the western Tianshan Mountains, NW China[J]. *Acta Petrologica Sinica*, 2006, 22 (5): 1341-1350 (in Chinese with English abstract).
- [41] Hofmann A W. Chemical differentiation of the earth: The relationship between large crust, and oceanic crust[J]. *Earth Planet Sci. Lett.*, 1988, 90: 297-314.
- [42] Green T H. Significance of Nb/Ta as an indicator of geochemical processes in the crust-mantle system[J]. *Chemical Geology*, 1995, 120: 347-359.
- [43] Taylor S R, McLennan S M. *The Continental Crust: Its Composition and Evolution* [M]. Oxford: Blackwell, 1985.
- [44] 王涛, 李伍平, 李金宝, 等. 东天山东段同造山到后造山花岗岩幔源组份的递增及陆壳垂向生长意义——Sr、Nd同位素证据[J]. *岩石学报*, 2008, 24(4): 762-772.  
Wang Tao, Li Wuping, Li Jinbao, et al. Increase of juvenile mantle-derived composition from syn-orogenic to post-orogenic granites of the west part of the eastern Tianshan (China) and implications for continental vertical growth: Sr and Nd isotopic evidence[J]. *Acta Petrologica Sinica*, 2008, 24(4): 762-772 (in Chinese with English abstract).
- [45] 韩宝福, 何国琦, 王式洸, 等. 新疆北部碰撞后幔源岩浆活动与陆壳纵向生长[J]. *地质论评*, 1998, 44, 396-409.  
Han Baofu, He Guoqi, Wang Shiguang, et al. Postcollisional Mantle-Derived Magmatism and Vertical Growth of the Continental Crust in North Xinjiang[J]. *Geological Review*, 1998, 44, 396-409 (in Chinese with English abstract).

- [46] Han B F, Wang S G, Jahn B M, et al. Depleted-mantle magma source for the Ulungur River A-type granites from north Xinjiang China: Geochemistry and Nd-Sr isotopic evidence, and implication for Phanerozoic crustal growth[J]. Chem. Geol. 1997, 138: 135-159.
- [47] Wu F Y, Jahn B M, Wilde S A, et al. Phanerozoic crustal growth: U-Pb and Sr-Nd isotopic evidence from the granites in northeastern China[J]. Tectonophysics, 2000, 328:89-113.
- [48] Wu F Y, Jahn B M, Wilde S A, et al. Highly fractionated I-type granites in NE China (II): isotopic geochemistry and implications for crustal growth in the Phanerozoic[J]. Lithos, 2003b, 67, 191-204.
- [49] Wang T, Zheng Y D, Li T B, et al. Mesozoic granitic magmatism in extensional tectonics near the Mongolian border in China and its implications for crustal growth[J]. Journal of Asian Earth Sciences, 2004, 23(5): 715-729.
- [50] Windley B F, Kroner A, Guo J H, et al. Neoproterozoic to Paleozoic geology of the Altai orogen, NW China[J]. The Journal of Geology, 2002, 110 (6): 719-737.
- [51] Xiao W J, Windley B F, Huang B C, et al. End-Permian to Mid-Triassic termination of the accretionary processes of the southern Altaids: implications for the geodynamic evolution, Phanerozoic continental growth, and metallogeny of central Asia[J]. International Journal of Earth Sciences, 2009, 98(6): 1189-1217.
- [52] Jahn B M, Wang T and Litvinovsky B A. Crustal growth in the Central Asian orogenic belt (the Altaids): Nd isotope evidence[J]. Geochimica et Cosmochimica Acta, 2006, 70 (8): A287-287.
- [53] Coleman R G. Continental growth of Northwest China[J]. Tectonics, 1989, 8: 521-635.
- [54] 洪大卫, 王式洸, 谢锡林, 等. 兴蒙造山带正 $\epsilon_{Nd}(t)$ 值花岗岩的成因和大陆地壳生长[J]. 地学前缘, 2000, 7: 41-45.  
Hong Dawei, Wang Shiguang, Xie Xilin, et al. Genesis of positive $\epsilon_{Nd}(t)$  granitoids in the Da Hinggan Mts.-Mongolia orogenic belt and growth continental crust[J]. Earth Science Frontiers, 2000, 7: 41-45 (in Chinese with English abstract).
- [55] Hong D W, Wang S G, Xie X L, et al. Continental crustal growth and the supercontinental cycle: evidence from the Central Asian Orogenic Belt[J]. Journal of Asian Earth Science, 2004, 23, 799-813.
- [56] 吴福元, 江博明, 林强, 等. 中国北方造山带造山后花岗岩的同位素特点与地壳生长意义[J]. 科学通报, 1997, 42: 2188-2192.  
Wu Fuyuan, Jahn Borming, Lin Qiang, et al. The later granites isotopic characteristic and continental crustal growth at Northern Belt in China [J]. Chinese Science Bulletin, 1997, 42: 2188-2192 (in Chinese).
- [57] 吴华, 李华芹, 莫新华, 等. 新疆哈密白石泉铜镍矿区基性-超基性岩的形成时代及其地质意义[J]. 地质学报, 2005, 79(4):498-502.  
Wu Hua, Li Huaqin, Mo Xinhua, et al. Age of the Baishiquan mafic-ultramafic complex, Hami, Xinjiang and its geological significance[J]. Acta Geologica Sinica, 2005, 79(4):498-502 (in Chinese with English abstract).
- [58] 李锦轶, 宋彪, 王克卓, 等. 东天山吐哈盆地南缘二叠纪幔源岩浆杂岩: 中亚地区陆壳垂向生长的地质记录[J]. 地球学报, 2006, 27(5):424-446.  
Li Jinyi, Song Biao, Wang Kezhao, et al. Permian Mafic-Ultramafic Complexes on the Southern Margin of the Tu-Ha Basin, East Tianshan Mountains: Geological Records of Vertical Crustal Growth in Central Asia[J]. Acta Geoscientia Sinica, 2006, 27(5): 424-446 (in Chinese with English abstract).
- [59] 舒良树, 朱文斌, 王博, 等. 新疆博格达南缘后碰撞期陆内裂谷和地下水滑塌构造[J]. 岩石学报, 2005, 21 (1): 25-36.  
Shu Liangshu, Zhu Wenbin, Wang Bo, et al. The post-collision intracontinental rifting and olistostrome on the southern slope of Bogda Mountains, Xinjiang[J]. Acta Petrologica Sinica, 2005, 21 (1): 25-36 (in Chinese with English abstract).
- [60] 胡远清, 廖群安, 施文翔, 等. 中天山路白山一带晚石炭世I型和A型花岗岩组合的厘定及其意义[J]. 地质科技情报, 2009, 28 (3): 10-18.  
Hu Yuanqing, Liao Qunan, Shi Wenxiang, et al. Determination and the geological significances of the Late Carboniferous I-type and A-type Granites from Middle Tianshan Block, East Tianshan district, NW China[J]. Geological Science and Technology Information, 2009, 28(3): 10-18 (in Chinese with English abstract).
- [61] Wu F Y, Simon A W, Zhang G L, et al. Geochronology and petrogenesis of the post-orogenic Cu-Ni sulfide-bearing mafic-ultramafic complexes in Jilin Province, NE China[J]. Journal of Asian Earth Sciences, 2004, 23, 781-797.